



Effect of serpentine and sodium hexametaphosphate on ascharite flotation

Zhi-hang LI, Yue-xin HAN, Yan-jun LI, Peng GAO

School of Resources and Civil Engineering, Northeastern University, Shenyang 110819, China

Received 23 June 2016; accepted 15 December 2016

Abstract: Sodium hexametaphosphate (SHMP) was used to minimize the adverse effect of serpentine for improving ascharite recovery. The effects of particle size and content of SHMP, and serpentine on ascharite flotation process were investigated through flotation, zeta potential tests, FT-IR analysis, XPS analysis and DLVO theory. Particles interaction and mechanism of SHMP were also discussed. It was found that aggregation between serpentine and ascharite particles easily happened, and the particle size of serpentine had a profound impact on the ascharite recovery. In particular, the fine serpentine with size less than 38 μm had the greatest contribution to the deterioration of ascharite flotation performance. After SHMP treatment, the adverse effect of serpentine was significantly reduced. The mechanism of SHMP showed that it could alter the surface charges of serpentine and ascharite to prevent severe interparticle aggregation, which resulted in a well-dispersed pulp and benefited ascharite flotation process. The adsorption of SHMP on serpentine was due to hydrogen bonding and chemical adsorption, resulting in the formation of complex on serpentine surface to decrease its floatability.

Key words: serpentine; ascharite; sodium hexametaphosphate; flotation; DLVO theory; interaction; adsorption

1 Introduction

The main boron mineral resources in China are ascharite ore and paigeite ore. After decades of exploitation, directly available ascharite resources are nearly exhausted and cannot meet the future needs of boron chemical production [1,2]. Therefore, it is crucial to exploit and utilize the less appealing paigeite resources to maintain a steady supply for the boron industry. Paigeite ore is rich in Dandong region, Liaoning province, China. The main valuable mineral in paigeite is ascharite and the main gangue mineral is serpentine closely associated with ascharite [3]. However, the dissemination sizes of serpentine are very fine and serpentine is prone to form slime during mineral processing, leading to a problem in flotation separation of ascharite from serpentine.

Pervious researches have shown that particle size has a great influence on particles interaction and interferes flotation performance significantly [4,5]. For instance, it is found that fine particle serpentine has adverse effects on flotation of nickel-bearing pyrite and

chromite [6,7]. Because of the difference on surface charge, fine serpentine particles can be adsorbed to the nickel-bearing pyrite and chromite easily, which leads to a low recovery of target mineral [8]. Sodium hexametaphosphate (SHMP) is found to be a good inhibitor to antigorite, which is one of important mineral polymorphs of serpentine. Moreover, SHMP can be adsorbed on the surfaces of the antigorite, diminishing the chance of the anionic collector adsorption [9]. Nevertheless, so far few studies have been found on the flotation separation of ascharite from serpentine. The influence of serpentine particles on ascharite flotation and the flotation behavior have not been studied systematically. Besides, the mechanism of SHMP is not fully understood.

In this study, the subjects that previous studies seldom discussed were carefully investigated. The influences of particle size and content of serpentine on ascharite flotation process were studied. The particles interaction between serpentine and ascharite was also systematically discussed. SHMP was used to diminish the detrimental effect of serpentine on ascharite flotation. The mechanism of SHMP was investigated to provide

insights to the ascharite flotation process. A better understanding of the flotation performance of ascharite in the presence of serpentine is essential for the future exploitation of paigeite resources and the mechanism of SHMP discussed in this research provides a reference for further study.

2 Experimental

2.1 Characterization of ascharite and serpentine samples

The serpentine and ascharite samples used in the experiments were obtained from Xiuyan and Dandong, Liaoning province, China. The ascharite was obtained by handpicking and then sieved to $<45\ \mu\text{m}$. A batch of serpentine rocks were first ground and sieved, then three products with different particle sizes were obtained, i.e., coarse ($45\text{--}74\ \mu\text{m}$), medium ($38\text{--}45\ \mu\text{m}$) and fine ($<38\ \mu\text{m}$). The particle size distribution is listed in Table 1. The chemical analyses of samples were also performed and shown in Table 2. X-ray diffraction patterns are shown in Fig. 1. The results demonstrated that serpentine and ascharite samples with purities of 95.6% and 94.5% respectively could meet the requirement for following research.

Table 1 Particle size distribution of samples

Mineral	Grade	$D_{10}/\mu\text{m}$	$D_{50}/\mu\text{m}$	$D_{90}/\mu\text{m}$	Volume average diameter/ μm
Serpentine	45–74 μm (coarse)	33.8	69.9	128.3	75.9
	38–45 μm (medium)	17.7	42.2	77.8	45.1
	$<38\ \mu\text{m}$ (fine)	2.1	11.0	42.3	12.8
Ascharite		1.9	20.1	49.9	27.8

Table 2 Compositions of serpentine and ascharite (mass fraction, %)

Mineral	MgO	SiO ₂	CaO	B ₂ O ₃	Al ₂ O ₃
Serpentine	42.09	43.68	0.90	–	0.88
Ascharite	46.21	0.74	0.25	39.16	–

2.2 Chemical reagents

Analytical grade reagents dodecylamine and SHMP were used as a collector for ascharite and an inhibitor for serpentine, respectively. Dilute solution of hydrochloric acid (HCl) and sodium hydroxide (NaOH) were employed as pH adjustment agents. Analytical grade reagent potassium nitrate was used to maintain the ionic strength in zeta potential measurement. The distilled water produced by automatic adsorption-type ultrapure water systems was used.

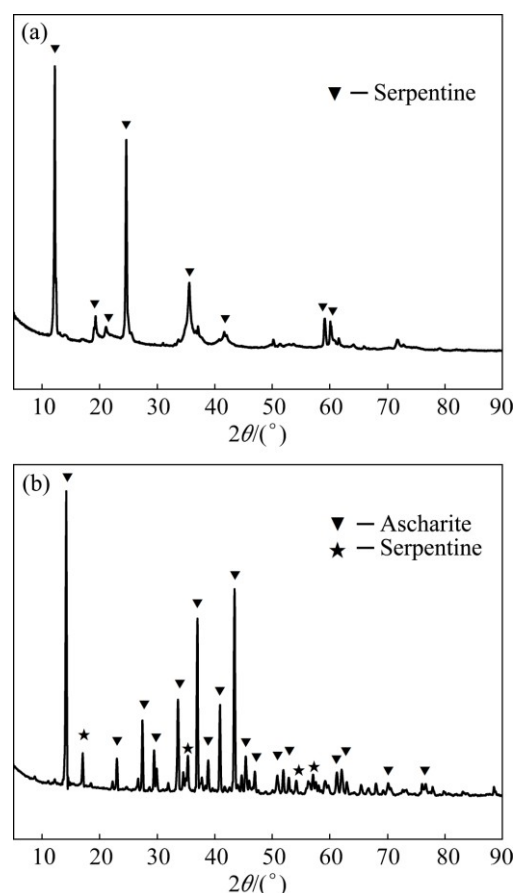


Fig. 1 XRD patterns of samples: (a) Serpentine; (b) Ascharite

2.3 Methods

2.3.1 Flotation tests

Flotation tests were carried out on an XFG flotation machine (30-mL cell and the impeller speed of 1920 r/min). Single mineral experiments were first performed to evaluate flotation performance of serpentine and ascharite, individually. Then, experiments of mixed minerals were carried out. A typical flotation test included the following steps: 1) weigh 2.0 g ascharite or serpentine in single mineral experiments; weigh a mixture of serpentine and ascharite at different mixing ratios (0.1:1, 0.3:1, 0.5:1, 0.8:1, 1:1, mass ratio of serpentine to ascharite) in mixed minerals experiments and keep the mass of ascharite constant (1.0 g); 2) place the mineral samples into the flotation cell, add with 30 mL deionized water, stir for 3 min and maintain the pulp at 20 °C; 3) add HCl and NaOH to achieve required pH value (pH=9.0); 4) add a predetermined dose of SHMP (0.65×10^{-4} mol/L) to the pulp and agitate for 3 min; 5) add a predetermined dose of the collector (3.2×10^{-4} mol/L), agitate for 3 min and collect the flotation froth for another 3 min. The froth products and tailings were dried, weighed and analyzed to calculate flotation recovery.

2.3.2 Zeta potential measurement

Isoelectric point values of serpentine and ascharite were measured by Malvern Zetasizer Nano potential meter. Initially, the mineral samples were ground to $<2\ \mu\text{m}$ and then 20 mg of serpentine or ascharite sample was added into 50 mL deionized water. Potassium nitrate was used to maintain the ionic strength at $1 \times 10^{-3}\ \text{mol/L}$. The suspension was magnetically stirred for 10 min and the pH value was adjusted with HCl and NaOH. The pH values of the suspension were recorded using a pH-3C pH meter. After that, the supernatant was measured with the potential meter 20 min later.

2.3.3 Infrared spectra analysis

The measurements were performed using a FT-IR spectrometer (NEXUS670). Before the test, the samples of SHMP, serpentine, and serpentine treated with SHMP ($0.65 \times 10^{-4}\ \text{mol/L}$) were all ground to $<2\ \mu\text{m}$. Then, 1.0 mg sample was mixed with 100.0 mg potassium bromide uniformly to prepare the powder pies needed for FT-IR spectrometer.

2.3.4 X-ray photoelectron spectroscopy measurement

The XPS spectra were measured with America Thermo VG ESCALAB250 spectrometer using Al K_{α}

X-ray (1486.6 eV) as sputtering source at a power of 150 W (15 kV \times 10 mA). The measurements were performed inside the analysis chamber operated at a high vacuum of $5.0 \times 10^{-7}\ \text{Pa}$. A value of 1304.7 eV was adopted as the standard Mg 1s to calibrate binding energy.

3 Results and discussion

3.1 Influence of serpentine content and particle size on ascharite flotation

Without SHMP addition, the recoveries of ascharite and serpentine in concentrate are presented in Figs. 2(a) and (b). It was evident that mixing ratio had an impact on ascharite recovery. With the increase of serpentine content, ascharite recoveries decreased accordingly. Moreover, the impacts of serpentine on ascharite recovery varied with the particle size of serpentine. For instance, the increase of coarse serpentine (45–74 μm) had little effect on ascharite recovery, while the increase of fine serpentine ($<38\ \mu\text{m}$) led to a sharp decrease of ascharite recovery from 92.5% to 17.6% (Fig. 2(a)). The impact of medium serpentine (38–45 μm) on ascharite

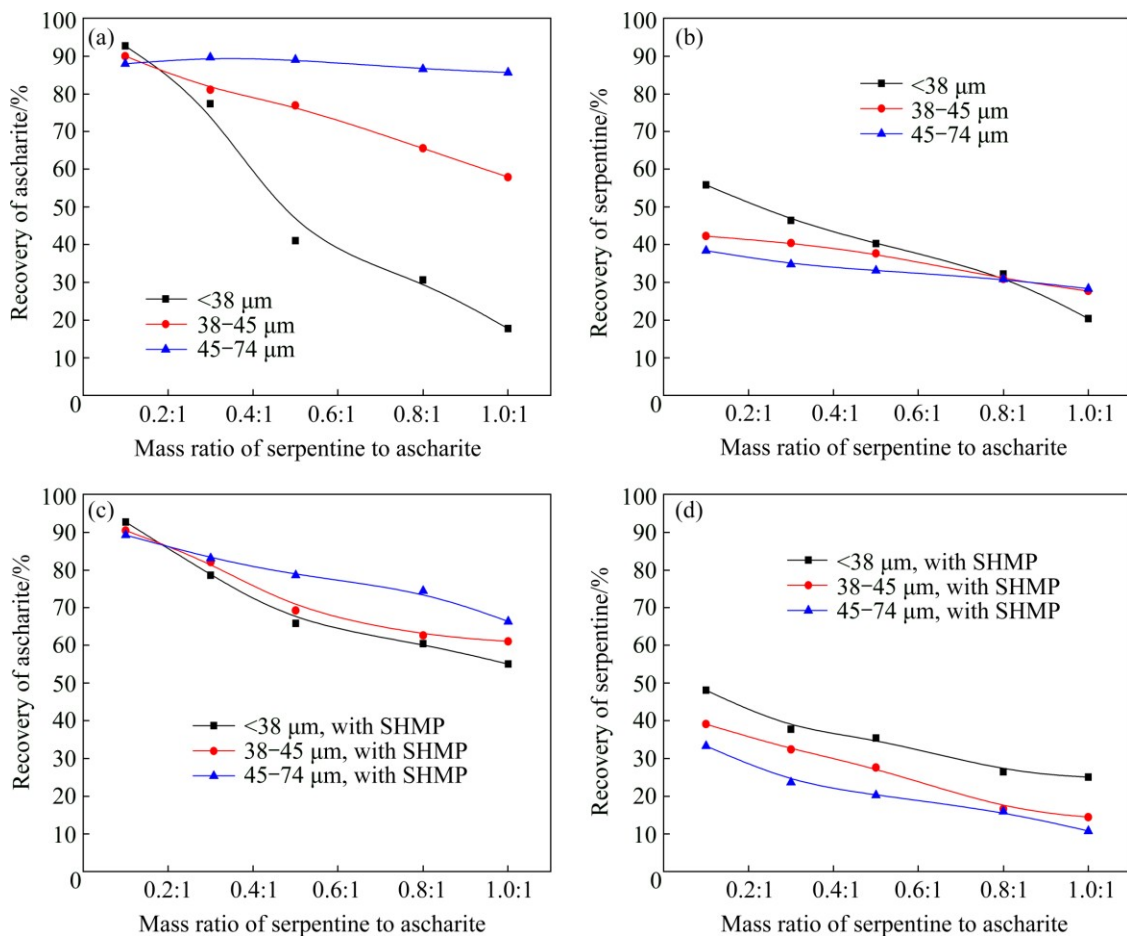


Fig. 2 Effects of content and particle size of serpentine on flotation recovery: (a) Recovery of ascharite without SHMP; (b) Recovery of serpentine without SHMP; (c) Recovery of ascharite with SHMP; (d) Recovery of serpentine with SHMP

recovery was mild. Consequently, although both serpentine content and particle size interfered with ascharite flotation recovery, the impact of particle size was more conspicuous. Meanwhile, the fine serpentine (<38 μm) showed a higher recovery in ascharite concentrate (Fig. 2(b)), which further confirmed the interference of fine serpentine was more obvious in the flotation process.

3.2 Influence of SHMP on ascharite flotation

To reduce the serpentine interference on ascharite flotation, SHMP was added to the pulp. As shown in Fig. 2(c), after SHMP treatment, the impact of fine serpentine (<38 μm) on ascharite flotation decreased significantly and ascharite recovery increased remarkably. Meanwhile, serpentine recovery in concentrate decreased. Moreover, recovery of ascharite mixed with coarse serpentine (45–74 μm) had a slight decrease, which indicated that SHMP depressed both serpentine and ascharite during flotation process (Figs. 2(c) and (d)), but the depression effect of SHMP on ascharite was not as effective as that on serpentine, and SHMP affected fine serpentine much more effectively than coarse serpentine.

This could be caused by the dose effect of SHMP. In order to further investigate the adsorption of SHMP on serpentine particles, the residual concentration of P in serpentine pulp with different particle sizes was detected and shown in Fig. 3. Figure 3 showed that SHMP could be absorbed on serpentine and most of SHMP could be absorbed on fine serpentine. For the equal mass of serpentine particles, the fine serpentine contained more particles and had larger total surface area for SHMP to absorb, thus leading to dose decrease of SHMP in aqueous solution.

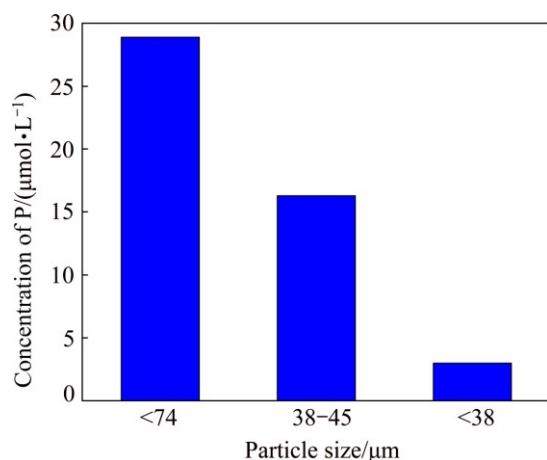


Fig. 3 Residual concentration of P in serpentine pulp with different particle sizes

3.3 Effects of pH on flotation and SHMP on zeta potentials of serpentine and ascharite

Figure 4(a) shows significant effects of pH value on

the flotation recoveries of serpentine and ascharite. The ascharite exhibited good floatability with the highest recovery of 85.4% at pH 9.0. In contrast, the highest recovery of serpentine was under 40% at pH 9.0. The poor floatability of serpentine was mostly due to its strong hydrophilicity.

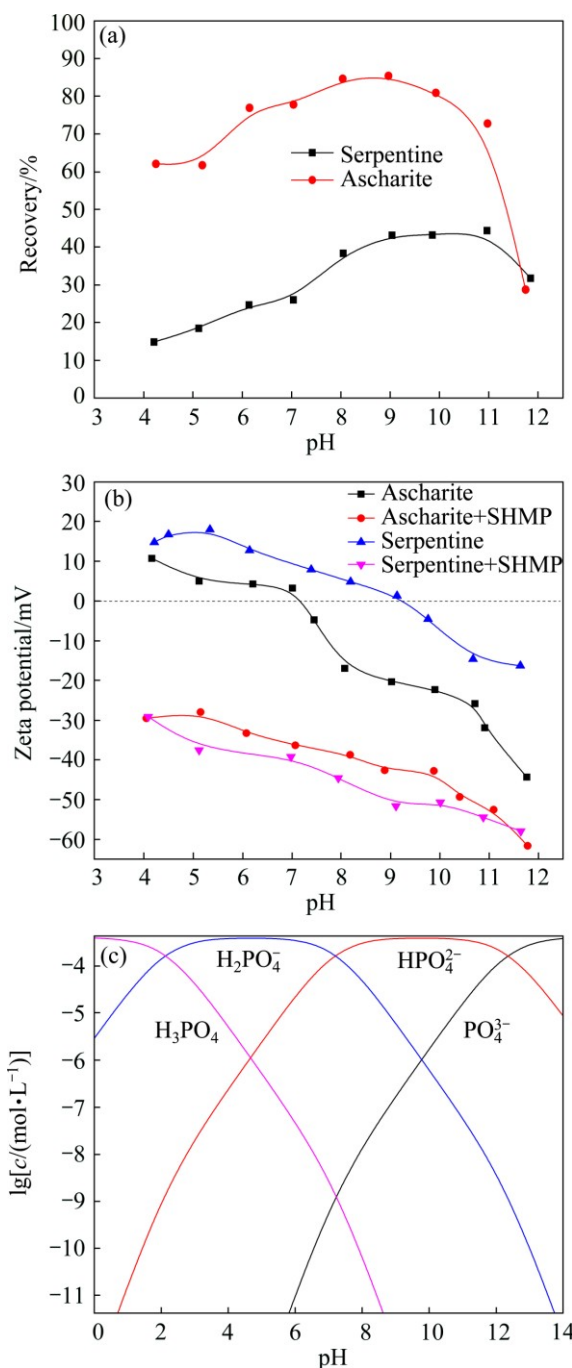
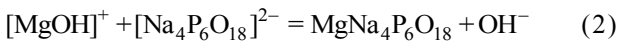
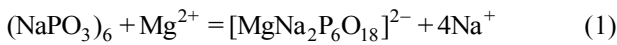


Fig. 4 Relationship between pH and flotation recovery (a), zeta potential (b) and species distribution (c)

Zeta potential analysis was widely used to interpret the flotation performance and the trend of flotation efficiency caused by reagents [10,11]. The zeta potentials of samples with SHMP or without SHMP treatment were depicted in Fig. 4(b). The pH values at the isoelectric

point for ascharite and serpentine were 7.3 and 9.2, respectively. SHMP had a significant influence on zeta potential. According to the speciation diagram of SHMP at a concentration of 0.65×10^{-4} mol/L (Fig. 4(c)), SHMP existed in the form of HPO_4^{2-} , H_2PO_4^- and PO_4^{3-} at pH 9.0. Based on the previous literatures [12,13], SHMP had a good complexation ability with metal ions, such as Ca^{2+} and Mg^{2+} , and the complexes were hydrophilic. As there were Mg^{2+} ions on the surface of serpentine and ascharite, SHMP could be absorbed on the surface of minerals. Therefore, the negative charges on the surface of minerals increased, which lowered the zeta potentials of serpentine and ascharite. The reaction process can be expressed as follows:



Furthermore, because surface charges of serpentine and ascharite were opposite in the pH range of 7.3–9.2, aggregation was prone to occur between serpentine and ascharite particles in the pulp. In the presence of SHMP, the surface charge of both serpentine and ascharite changed from positive to negative in the whole pH range and SHMP rendered serpentine much more electronegative than ascharite. Therefore, the aggregation between serpentine and ascharite particles was mitigated by SHMP.

3.4 Particles interaction between serpentine and ascharite

The experiment results indicated that serpentine influenced ascharite flotation results significantly. This might be caused by particles interaction, which led to fine serpentine particles adhering to ascharite particles. Based on the DLVO theory [14,15], the total energy V_T between serpentine particles and ascharite particles could be described as

$$V_T = V_W + V_E \quad (3)$$

where V_T , V_W and V_E are the total energy, Vander Waals energy and electrostatic energy, respectively; V_W can be calculated as

$$V_W = -\frac{AR_1R_2}{6H(R_1 + R_2)} \quad (4)$$

and

$$A = (\sqrt{A_{11}} - \sqrt{A_{33}})(\sqrt{A_{22}} - \sqrt{A_{33}}) \quad (5)$$

where the Hamaker constant of serpentine A_{11} is 10.6×10^{-20} J, the Hamaker constant of ascharite A_{22} is 19.3×10^{-20} J, the Hamaker constant of water A_{33} is 4.15×10^{-20} J [16,17]; R_1 and R_2 are radii of serpentine particles and ascharite particles, respectively. H represents the distance between particles, nm; A

represents the effective Hamaker constant for serpentine and ascharite in aqueous solution; electrostatic energy can be expressed as

$$V_E = \frac{\pi\epsilon_a R_1 R_2}{R_1 + R_2} (\phi_1^2 + \phi_2^2) \left(\frac{2\phi_1\phi_2}{\phi_1^2 + \phi_2^2} \times \ln\left(\frac{1 + \exp(-\kappa H)}{1 - \exp(-\kappa H)}\right) + \ln(1 - \exp(-\kappa H)) \right) \quad (6)$$

where κ is the reciprocal of thickness of electric double-layer, $\kappa = 0.180 \text{ nm}^{-1}$ [18]; ϵ_a is the relative dielectric constant of the continuous phase; ϕ_1 and ϕ_2 are surface potentials, mV. A dynamic potential can be used. The results are shown in Fig. 5.

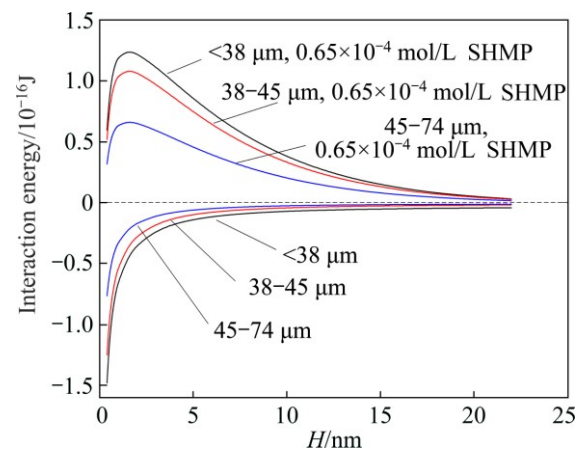


Fig. 5 Relationship of interaction energy between serpentine and ascharite particles

In Fig. 5, the total interaction energy between serpentine and ascharite particles without SHMP was negative. So, aggregation occurred easily between serpentine and ascharite particles. Moreover, the total energy between fine serpentine (<38 μm) and ascharite particles was most negative, so the fine serpentine particles were more likely to adhere to ascharite. As aforementioned, the floatability of serpentine was poor. When fine serpentine particles adhered to ascharite, the floatability of ascharite was compromised. With the increase of serpentine content, more fine serpentine particles adhered to ascharite, thus the adverse effect of serpentine on ascharite was enhanced and ascharite recovery decreased rapidly. Meanwhile, due to the aggregation, a portion of fine serpentine particles were more likely to float together with ascharite, resulting in a high serpentine recovery. It explained why the recovery of fine serpentine was the highest in concentrates.

With the addition of SHMP, the total energy between serpentine and ascharite changed from negative to positive, where mutual exclusion appeared and the aggregation was mitigated. Figure 5 also showed that SHMP had a better effect on dispersing fine serpentine

with ascharite. Therefore, the recovery of ascharite mixed with fine serpentine ($<38\ \mu\text{m}$) increased greatly after being treated with SHMP. Meanwhile, the serpentine recoveries were lowered compared with the results without adding SHMP.

3.5 FT-IR spectra analysis

In order to verify the adsorption of SHMP on surface of serpentine, the FT-IR spectrum of serpentine after SHMP treatment is obtained in Fig. 6.

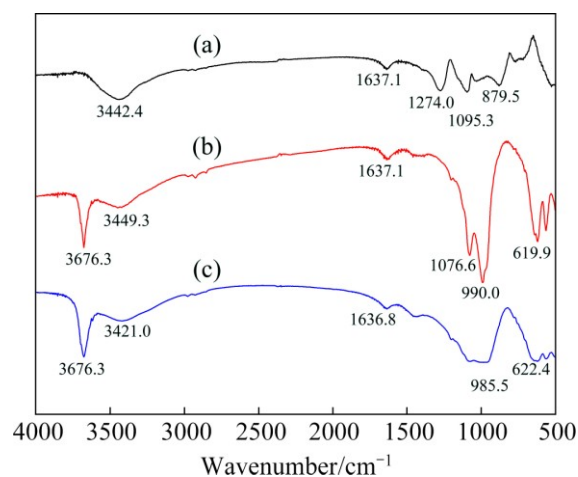


Fig. 6 FT-IR spectra of samples: (a) SHMP; (b) Serpentine; (c) Serpentine treated with SHMP

In the infrared spectrum of SHMP, the peaks at 1274.0 , 1095.3 and $879.5\ \text{cm}^{-1}$ corresponded to the characteristic peaks of $\text{P}=\text{O}$, $\text{P}-\text{O}$ and $\text{P}-\text{O}-\text{P}$, respectively [19]. In the spectrum of serpentine, the characteristic sharp bands at 1076.6 and $990.0\ \text{cm}^{-1}$ were due to the stretching vibration of $\text{Si}-\text{O}$ group [20]. The characteristic sharp band at $3449.3\ \text{cm}^{-1}$ in the spectrum was due to $-\text{OH}$ [21]. In the infrared spectrum of serpentine after SHMP treatment at pH value of 9.0, the characteristic peak of serpentine at $3449.3\ \text{cm}^{-1}$ corresponding to $-\text{OH}$ vibration shifted to a lower frequency of $3421.0\ \text{cm}^{-1}$. It can be concluded that $-\text{OH}$ group was involved in the adsorption process and therefore hydrogen bonding adsorption occurred, indicating that SHMP changed the surface hydroxyl of serpentine [22,23]. Compared with the spectrum of serpentine itself, the bond shift of peak at $1095.3\ \text{cm}^{-1}$ on curve (c) was strengthened after SHMP treatment, which also indicated that SHMP was adsorbed onto the surfaces of serpentine.

3.6 XPS analysis

The XPS analysis results of serpentine treated and untreated with SHMP are shown in Fig. 7. In the XPS spectrum of serpentine, the C 1s peak at 284.6 eV was due to surface contaminants formed by air exposure of

the sample [24]. The peak at 532.5 and 101.9 eV corresponded to oxygen and silicon presence, respectively. In addition, the Mg 1s peak at 1304.7 eV was confirmed from the spectrum and no other peaks were detected on serpentine surface, which verified that the serpentine was relatively pure and unpolluted. In the spectrum of serpentine treated with SHMP, a small and new peak near 132.9 eV corresponding to P 2p of SHMP was detected. However, no remarkable peaks were found in XPS spectrum of serpentine untreated with SHMP at the same point. This confirmed the adsorption of SHMP onto the serpentine surface.

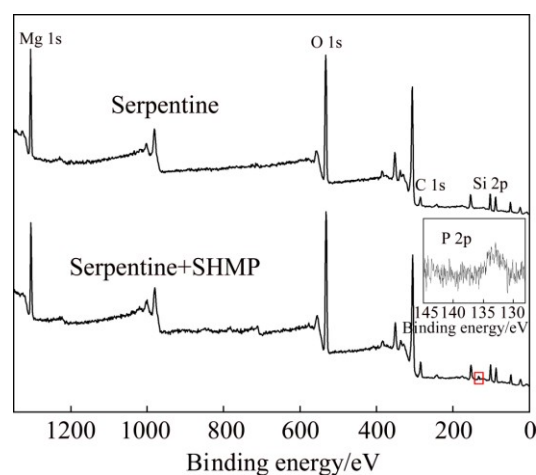


Fig. 7 XPS spectra of serpentine treated and untreated with SHMP

In order to further investigate the adsorption mechanism of SHMP on serpentine, results of the spectra are listed in Table 3. Compared with initial serpentine surface, P 2p adsorption on the surface was found with an increase of O 1s content and decrease of Mg 1s and Si 2p contents. Besides, the Mg 1s peak on serpentine treated with SHMP was analyzed by peak fitting, as shown in Fig. 8. The result unveiled that spectra consisted of two new components at 1302.7 and 1303.9 eV, which could be assigned to Mg 1s peaks in $\text{Mg}-\text{O}$ and $\text{Mg}-\text{OH}$ [25,26]. The Mg 1s peak shifting toward lower binding energy confirmed the adsorption of SHMP on serpentine surface by chemical adsorption.

Table 3 XPS characterization of samples

Sample	Mole fraction/% or (Binding energy/eV)				
	C	O	Mg	Si	P
Serpentine	8.73 (284.6)	53.69 (532.5)	21.97 (1304.7)	15.61 (101.9)	
Serpentine+ SHMP	14.47 (284.6)	53.95 (532.5)	12.88 (1304.6) 2.61 (1302.7) 1.24 (1303.9)	14.36 (101.8)	0.48 (132.9)

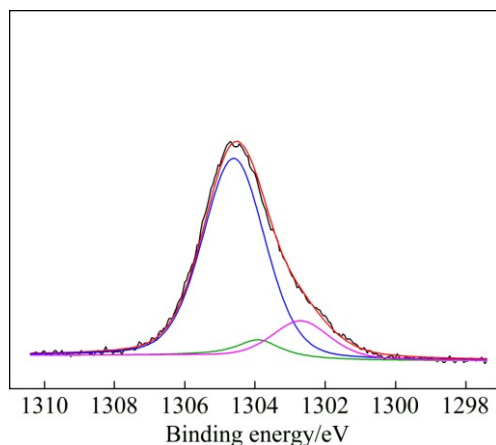


Fig. 8 XPS Mg 1s spectra of serpentine treated with SHMP

4 Conclusions

1) Compared with ascharite, the floatability of serpentine is poor. Serpentine affects ascharite recovery obviously. The smaller particle size and higher content of serpentine can lead to a lower ascharite recovery. Although both serpentine content and particle size could interfere with ascharite recovery, the effect of serpentine particle size was more remarkable.

2) Because of the surface charge difference on minerals surfaces, aggregation occurs between serpentine and ascharite particles. The fine serpentine particles exhibit high tendency adhering to ascharite. After SHMP treatment, surface charge of both serpentine and ascharite are changed to be negative, which mitigates the heterogeneous aggregation effectively.

3) SHMP can be adsorbed on the surface of serpentine via hydrogen bonding and chemical adsorption, and most of SHMP can be adsorbed on fine serpentine surface. The effect of SHMP on dispersing fine serpentine particles ($<38 \mu\text{m}$) with ascharite is effective, but dispersion effect of SHMP on serpentine $>38 \mu\text{m}$ is not obvious. After SHMP treatment, the recovery of ascharite in the presence of fine serpentine ($<38 \mu\text{m}$) increases significantly.

References

- [1] DUAN Hua-mei, LÜ Xiao-shu, NING Zhi-qiang, ZHAI Yu-chun. Boron extraction from boron-concentrate ore by ammonium sulfate roasting method [J]. *Journal of Northeastern University (Natural Science)*, 2011, 32(12): 1724–1728. (in Chinese)
- [2] ZHANG Li-qing, YUAN Ben-fu, ZHOU Hua-feng, LIU Zhi-guo. Extracting magnesium sulfate from acid-leaching solution of ludwigite by ethanol crystallization [J]. *Journal of Central South University (Science and Technology)*, 2013, 44(7): 2681–2687. (in Chinese)
- [3] LI Yan-jun, HAN Yue-xin, ZHU Yi-min. Study on the characteristic of camsellite flotation [J]. *Journal of Northeastern University (Natural Science)*, 2007, 28(7): 1041–1044. (in Chinese)
- [4] FENG Bo, LU Yi-ping, FENG Qi-ming, ZHANG Ming-yang, GU Yan-ling. Talc-serpentine interactions and implications for talc depression [J]. *Minerals Engineering*, 2012, 32: 68–73.
- [5] FENG Bo, FENG Qi-ming, LU Yi-ping. A novel method to limit the detrimental effect of serpentine on the flotation of pentlandite [J]. *International Journal of Mineral Processing*, 2012, 114: 11–13.
- [6] ZHOU Xiao-wen, FENG Bo. The effect of polyether on the separation of pentlandite and serpentine [J]. *Journal of Materials Research and Technology*, 2015, 4(4): 429–433.
- [7] GALLIOS G P, DEHYANNI E A, PELEKA E N, MATIS K A. Flotation of chromite and serpentine [J]. *Separation and Purification Technology*, 2007, 55(2): 232–237.
- [8] FENG Bo, LU Yi-ping, LUO Xian-ping. The effect of quartz on the flotation of pyrite depressed by serpentine [J]. *Journal of Materials Research and Technology*, 2015, 4(1): 8–13.
- [9] XIA Qi-bin, LI Zhong, QIU Xian-yang, DAI Zi-lin. Investigation of action mechanism between sodium hexametaphosphate and serpentine [J]. *Mining and Metallurgical Engineering*, 2002, 22(2): 51–54. (in Chinese)
- [10] LUO Bin-bin, ZHU Yi-min, SUN Chuan-yao, HAN Yue-xin. Flotation and adsorption of a new collector alpha-bromodecanoic acid on quartz surface [J]. *Minerals Engineering*, 2015, 77: 86–92.
- [11] ALVAREZ-SILVA M, URIBE-SALAS A, WATERS K E, FINCH J A. Zeta potential study of pentlandite in the presence of serpentine and dissolved mineral species [J]. *Minerals Engineering*, 2016, 85: 66–71.
- [12] FENG Qi-ming, ZHOU Qing-bo, ZHANG Guo-fan, LU Yi-ping, YANG Shao-yan. Inhibition mechanism of sodium hexametaphosphate on calcite [J]. *The Chinese Journal of Nonferrous Metals*, 2011, 21(2): 436–441. (in Chinese)
- [13] FENG Bo, LU Yi-ping, FENG Qi-ming, DING Peng, LUO Na. Mechanisms of surface charge development of serpentine mineral [J]. *Transactions of Nonferrous Metals Society of China*, 2013, 23(4): 1123–1128.
- [14] WANG Chong-qing, WANG Hui, GU Guo-hua, FU Jian-gang, LIN Qing-quan, LIU You-nian. Interfacial interactions between plastic particles in plastics flotation [J]. *Waste Management*, 2015, 46: 56–61.
- [15] de MESQUITA L M S, LINS F F, TOREM M L. Interaction of a hydrophobic bacterium strain in a hematite–quartz flotation system [J]. *International Journal of Mineral Processing*, 2003, 71: 31–44.
- [16] ZHAO Rui-chao, HAN Yue-xin, YANG Guang, LI Yan-jun. Mechanism of adsorption and aggregation of fine siderite, quartz and hematite [J]. *Journal of Northeastern University (Natural Science)*, 2015, 36(4): 596–600. (in Chinese)
- [17] YIN Wan-zhong, WANG Ji-zhen. Effects of particle size and particle interactions on scheelite flotation [J]. *Transactions of Nonferrous Metals Society of China*, 2014, 24(11): 3682–3687.
- [18] LU Ji-wei, YUAN Zhi-tao, LIU Jiong-tian, LI Li-xia, ZHU Shuo. Effects of magnetite on magnetic coating behavior in pentlandite and serpentine system [J]. *Minerals Engineering*, 2015, 72: 115–120.
- [19] TAN Xin, HE Fa-yu, SHANG Yan-bo, YIN Wan-zhong. Flotation behavior and adsorption mechanism of (1-hydroxy-2-methyl-2-octenyl) phosphonic acid to cassiterite [J]. *Transactions of Nonferrous Metals Society of China*, 2016, 26(9): 2469–2478.
- [20] SAIKIA B J, PARTHASARATHY G, SARMAH N C. Fourier transform infrared spectroscopic estimation of crystallinity in SiO_2 based rocks [J]. *Bulletin of Materials Science*, 2008, 31(5): 775–779.
- [21] ZHU Yi-min, LUO Bin-bin, SUN Chuan-yao, LI Yan-jun, HAN Yue-xin. Influence of bromine modification on collecting property of lauric acid [J]. *Minerals Engineering*, 2015, 79: 24–30.

- [22] WANG Li, SUN Wei, HU Yue-hua, XU Long-hua. Adsorption mechanism of mixed anionic/cationic collectors in muscovite-quartz flotation system [J]. Minerals Engineering, 2014, 64: 44–50.
- [23] LU Yi-ping, ZHANG Ming-qiang, FENG Qi-ming, LONG Tao, OU Le-ming, ZHANG Guo-fan. Effect of sodium hexametaphosphate on separation of serpentine from pyrite [J]. Transactions of Nonferrous Metals Society of China, 2011, 21(1): 208–213.
- [24] LIU Wen-gang, LIU Wen-bao, WANG Xin-yang, WEI De-zhou, WANG Ben-ying. Utilization of novel surfactant N-dodecyl-isopropanolamine as collector for efficient separation of quartz from hematite [J]. Separation and Purification Technology, 2016, 162: 188–194.
- [25] MILCIUS D, GRBOVIC-NOVAKOVIC J, ZOSTAUTIENE R, LELIS M, GIRDZEVICIUS D, URBONAVICIUS M. Combined XRD and XPS analysis of ex-situ and in-situ plasma hydrogenated magnetron sputtered Mg films [J]. Journal of Alloys and Compounds, 2015, 647: 790–796.
- [26] JENSEN I J T, THOGERSEN A, LOVVIK O M, SCHREUDERS H, DAM B, DIPLAS S. X-ray photoelectron spectroscopy investigation of magnetron sputtered Mg–Ti–H thin films [J]. International Journal of Hydrogen Energy, 2013, 38(25): 10704–10715.

蛇纹石及六偏磷酸钠对硼镁石浮选的影响

李治杭, 韩跃新, 李艳军, 高 鹏

东北大学 资源与土木工程学院, 沈阳 110819

摘 要: 为提高硼镁石浮选回收率, 使用六偏磷酸钠减小蛇纹石对浮选的不利影响。通过浮选试验、zeta 电位测试、傅里叶红外光谱分析、XPS 分析及 DLVO 理论等手段, 研究蛇纹石粒度、含量以及六偏磷酸钠(SHMP)对硼镁石浮选的影响, 并对矿物颗粒间的相互作用以及六偏磷酸钠的作用机理进行分析。结果表明, 蛇纹石与硼镁石颗粒间易发生团聚作用, 且蛇纹石粒度对硼镁石浮选结果影响十分显著。与粗粒级蛇纹石相比, 粒径小于 38 μm 的蛇纹石能显著降低硼镁石的回收率。加入 SHMP 后, 蛇纹石对硼镁石浮选的不利影响得到明显减弱。机理研究表明, SHMP 能影响蛇纹石与硼镁石矿物表面电荷, 从而阻碍颗粒间团聚的发生, 使矿物颗粒在矿浆中呈良好的分散状态, 有利于硼镁石的浮选。此外, SHMP 通过氢键与化学吸附作用于蛇纹石表面, 并生成一种络合物使蛇纹石的可浮性降低。

关键词: 蛇纹石; 硼镁石; 六偏磷酸钠; 浮选; DLVO 理论; 相互作用; 吸附

(Edited by Wei-ping CHEN)